

MODIS On-board Blackbody Function and Performance

Xiaoxiong (Jack) Xiong^a, Brian N. Wenny^b, Aisheng Wu^b, and William Barnes^c

^aSciences and Exploration Directorate, NASA/GSFC, Greenbelt, MD 20771;

^bScience Systems and Applications, Inc., 10210 Greenbelt Road, Lanham, MD 20706;

^cUniversity of Maryland, Baltimore County, 1000 Hilltop Circle, Baltimore, MD 21250.

Abstract - Two MODIS instruments are currently in orbit, making continuous global observations in visible to long-wave infrared wavelengths. Compared to heritage sensors, MODIS was built with an advanced set of on-board calibrators, providing sensor radiometric, spectral, and spatial calibration and characterization during on-orbit operation. For the thermal emissive bands (TEB) with wavelengths from 3.7 μm to 14.4 μm , a v-grooved blackbody (BB) is used as the primary calibration source. The BB temperature is accurately measured each scan (1.47s) using a set of 12 temperature sensors traceable to NIST temperature standards. The on-board BB is nominally operated at a fixed temperature, 290K for Terra MODIS and 285K for Aqua MODIS, to compute the TEB linear calibration coefficients. Periodically, its temperature is varied from 270K (instrument ambient) to 315K in order to evaluate and update the nonlinear calibration coefficients. This paper describes MODIS on-board BB functions with emphasis on on-orbit operation and performance. It examines the BB temperature uncertainties under different operational conditions and their impact on TEB calibration and data product quality. The temperature uniformity of the BB is also evaluated using TEB detector responses at different operating temperatures. On-orbit results demonstrate excellent short-term and long-term stability for both the Terra and Aqua MODIS on-board BB. The on-orbit BB temperature uncertainty is

estimated to be 10mK for Terra MODIS at 290K and 5mK for Aqua MODIS at 285K, thus meeting the TEB design specifications. In addition, there has been no measurable BB temperature drift over the entire mission of both Terra and Aqua MODIS.

Key words: MODIS, on-board calibrators, blackbody, calibration, temperature stability

I. Introduction

Currently, there are two nearly identical MODIS instruments operated on-orbit, one on-board the Terra spacecraft launched in December 1999 and another on-board the Aqua spacecraft launched in May 2002. Since launch, both Terra and Aqua MODIS have been making continuous global observations which are used to generate a broad range of data products for studying changes in the Earth's system of land, oceans, and atmosphere [1]. Each MODIS makes observations in 36 spectral bands with wavelengths covering spectral regions from the visible (VIS) to long-wave infrared (LWIR). Bands 1-19 and 26 are the reflective solar bands (RSB), designed to measure the Earth view surface-reflected solar radiation (daytime only). Bands 20-25 and 27-36 make observations of the thermal emission from Earth view targets (daytime and nighttime) and are referred to as the thermal emissive bands (TEB). Key applications of MODIS spectral bands include land/cloud properties, ocean color and biochemistry, surface/cloud temperatures, and atmospheric water vapor [1-6]. To ensure and maintain its science data product quality, MODIS was designed with a set of state-of-the-art on-board calibrators (OBC) enabling sensor radiometric, spatial, and spectral calibration to be made and monitored over its entire mission. In order to establish on-orbit calibration and characterization traceability from ground-based references to the on-board calibrators, extensive pre-launch measurements were carried out by the instrument vendor for both Terra and Aqua MODIS [7-10]. MODIS on-orbit calibration capability is a major advance over its heritage sensors, such as AVHRR and Landsat Thematic Mapper (TM). MODIS OBC include a solar diffuser (SD), a solar diffuser stability monitor (SDSM), a blackbody (BB), a spectroradiometric calibration assembly (SRCA), and a space view (SV) port. The SD/SDSM system is used together for RSB calibration. The BB is designed for TEB calibration. The SRCA is primarily responsible for sensor spatial and spectral

stability characterization. In addition, the SV port provides measurements of the sensor's thermal background and electronics offset [11-16].

Typically, an on-board BB is used for the in-flight calibration of each detector (channel) of a sensor's thermal emissive bands. There are different types of on-board BB, including a honeycomb type used in the AVHRR and GLI and a cavity BB used in the ATSR, TM and AIRS [17-21]. MODIS uses a full aperture v-grooved BB as shown in Figure 1. MODIS, a cross-track scanning radiometer, collects data each scan from its OBC sectors (SD, SRCA, BB, and SV) and the Earth view (EV) sector. The TEB on-orbit calibration is performed on a scan-by-scan basis using a quadratic calibration algorithm which relates the on-board BB (calibration source) and SV (instrument background) temperature (radiance) to the sensor's digital response. Unlike typical BB operations in many heritage sensors, which have no temperature control capability, the MODIS BB can be set to any temperature between instrument ambient and 315K and can also be varied continuously within this range. This feature has significantly enhanced the sensor's capability of tracking and updating the TEB nonlinear calibration coefficients during its on-orbit operation.

The objective of this paper is to provide a quantitative evaluation of the MODIS BB on-orbit operation and performance, including its impact on the TEB calibration and the Level 1B (L1B) data product quality. Following a brief description of instrument background and key pre-launch calibration and characterization activities designed to evaluate the performance of the MODIS on-board BB (Section 2), an overview of BB on-orbit operation and calibration activities (Section 3) is presented. In Section 4, BB on-orbit performance and its impact on TEB radiometric calibration are discussed for both Terra and Aqua MODIS. Additional discussions, focusing on lessons learned from MODIS on-board BB operational performance and their

applications to future sensor designs are included in Section 5. Section 6 is a summary of this paper. Results derived from on-orbit measurements show that MODIS on-board BB temperature and temperature uniformity have been extremely stable. In general, the performance of Aqua MODIS BB is better than Terra MODIS BB. Typical BB temperature uncertainty, estimated from scan-by-scan variations, is about 10mK for Terra MODIS and 5mK for Aqua MODIS at their nominal operating temperatures. Furthermore, the BB temperature drift over the entire mission of each sensor has been extremely small.

II. Instrument Background

MODIS collects data in 36 spectral bands, which are located, according to their wavelengths, on four focal plane assemblies (FPA): visible (VIS), near infrared (NIR), short- and mid-wave infrared (SMIR), and long-wave infrared (LWIR). MODIS bands are aligned in the cross-track direction with detectors in each spectral band aligned in the along-track direction. The VIS and NIR FPA, which have no temperature control and thus vary with the instrument temperature, are referred to as the warm FPA. The SMIR and LWIR FPA are the cold FPA (CFPA) with their on-orbit temperatures nominally controlled at 83K. MODIS bands 1-19 and 26 are the reflective solar bands (RSB) with wavelengths from 0.41 to 2.2 μ m, covering the VIS, NIR, and SWIR spectral regions and making observations at three spatial resolutions (nadir): 0.25km (2 bands), 0.5km (5 bands), and 1km (13 bands). The remaining 16 spectral bands are the thermal emissive bands (TEB) with wavelengths from 3.75 to 14.24 μ m and spatial resolutions (nadir) of 1km. Bands 20-25 are located on the SMIR FPA and bands 27-36 on the LWIR FPA. There are a total of 160 TEB detectors (10 per band). Table 1 is a summary of key design requirements for the MODIS TEB. The TEB radiometric calibration requirements, noise

equivalent temperature difference (NE Δ T) and calibration uncertainty (UC), are defined at specified typical radiance levels (L_{typ}) for each spectral band. As shown in Table 1, most bands have a calibration uncertainty requirement of 1%. Exceptions are 0.5% for bands 31 and 32, and 0.75% for band 20. At any radiance between $0.3L_{typ}$ and $0.9L_{max}$ (L_{max} : specified maximum radiance), the absolute accuracy shall not exceed the above values by more than 1%. For band 21 (low gain), the calibration requirement is 10% when it is operated for fire detection at its L_{max} . MODIS is a scanning radiometer. It makes EV observations over a $\pm 55^\circ$ range about nadir. The above calibration requirements are applied to observations made within a $\pm 45^\circ$ range. In general, MODIS has much more stringent requirements than most heritage sensors.

In order to maintain data quality over its entire mission, an on-board BB was designed for the TEB calibration. To achieve this objective, extensive pre-launch calibration and characterization measurements were also made using a ground-based blackbody calibration source (BCS). The OBC BB, shown in Figure 1, is a v-grooved plate with its temperature measured using 12 temperature sensors (thermistors), which are embedded in the BB substrate in a rectangular array of 2 in the along track direction by 6 in the cross-track direction. Each thermistor was characterized pre-launch with traceability to NIST temperature standards. In addition to having NIST traceable temperature measurements, accurate knowledge of the spectral emissivity is critically important. Because of this, special effort was made during pre-launch measurements to characterize the OBC BB spectral emissivity by operating the BB concurrently with the ground-based BCS so that the sensor could collect simultaneous data from both targets. This allowed the OBC BB emissivity to be determined via reference to the ground-based BCS, which has an emissivity of better than 0.9999.

MODIS TEB pre-launch radiometric calibration was performed at different instrument temperature levels which were referred to as the cold, nominal, and hot plateaus, and at different CFPA temperatures. Most measurements were made at the nominal instrument plateau and with the CFPA temperature set at 83K. Two additional CFPA temperature settings (85K and 88K) are also available for both Terra and Aqua MODIS. During sensor thermal vacuum radiometric calibration, the BCS temperatures varied from 170K to 340K for TEB detector noise, dynamic range, and nonlinearity characterization. The OBC BB was operated at different temperatures for gain and offset characterization. Apart from being used as a calibration source for the TEB, the on-board BB also provides a reference for the detector DC restore (DCR), a function designed to adjust each detector's dynamic range. The DCR operation is executed on a scan-by-scan and detector-by-detector basis using pre-launch determined reference values for a range of BB temperatures.

The on-board BB was designed to be temperature controlled from instrument ambient to 315K via a pair of electrical heaters. The dynamic range of the OBC BB thermistors was carefully designed to cover this temperature range. Pre-launch measurements showed that all thermistors met this requirement. Figure 2(a) is a typical relationship of thermistor temperature as a function of electronic readout in digital numbers (DN), with higher BB temperatures related to lower resistance in the temperature sensor (low DN). For a 12-bit analog-to-digital (ADC) readout, the DN range from 0 to 4095. Table 2 is a summary of individual BB thermistor dynamic ranges for both Terra and Aqua MODIS, including cases when the BB is operated with the A-side and the B-side electronics (duplicate subsystems to provide redundancy). Figure 2(b) is the typical temperature resolution ($\Delta\langle T_{bb} \rangle$) of a BB thermistor at different digital number (DN) readouts where 1 DN is used to quantify the telemetry error. It should be pointed out that

the actual digitization error is generally smaller than 1 DN. Because of the nonlinear relationship between BB thermistor temperature and readout digital number as displayed in Figure 2(a), the same digitization error leads to a larger temperature error at a higher temperature (smaller DN) than at a lower temperature (larger DN). Based on pre-launch characterization, the calibration differences among individual thermistors was small and, therefore, no special effort was made to correct for these differences. During on-orbit calibration, the averaged temperature from all 12 thermistors is used as the representative temperature for the on-board BB. Using the average has significantly reduced the random errors due to telemetry noise from individual thermistors.

III. MODIS OBC BB On-orbit Operation and Application

During nominal on-orbit operation, the BB temperature is controlled at 290K for Terra MODIS and 285K for Aqua MODIS. This is because the majority of the pre-launch calibration and characterization measurements for the thermal emissive bands were made at 290K and 285K for Terra and Aqua MODIS, respectively. The BB heater on and off operation is controlled on a scan-by-scan basis. Periodically, a BB warm-up and cool-down (WUCD) operation is executed in order to acquire additional calibration information. During BB WUCD, the BB temperatures can be varied from instrument ambient to 315K. This is an enhanced feature compared to BB design and operation of other heritage sensors, in which the BB temperature floats passively with the instrument temperature without any temperature control capability. Figure 3 illustrates a typical BB WUCD operation for Terra MODIS (a) and Aqua MODIS (b) using BB temperatures from thermistor 1 (T_{bb1}) and the average of all 12 thermistors ($\langle T_{bb} \rangle$). From Figure 3, it is hard to discern any difference between T_{bb1} and $\langle T_{bb} \rangle$. A detailed analysis on the differences between

the temperatures retrieved from an individual thermistor (T_{bb}) and the average temperature ($\langle T_{bb} \rangle$) will be examined in the next section.

When the BB WUCD operation is executed, the BB temperature is first cooled from its nominal temperature (290K for Terra MODIS and 285K for Aqua MODIS) to the instrument ambient at approximately 270K by turning off the BB heater. After the BB temperature reaches instrument ambient, the warm-up process begins by enabling the BB heater. This is a carefully designed step-wise process. Instead of warming the BB continuously to its pre-defined maximum operating temperature at 315K, the BB is controlled, step-by-step, at several pre-determined intermediate levels (temperatures). This operation allows detector response and noise characterization to be examined at multiple well-controlled radiance levels or temperatures. Shortly after the BB temperature reaches 315K, the heater is disabled again. This provides a complete BB cool-down data set with the BB temperature continuously changing from its maximum (315K) to minimum (instrument ambient). This data set is used to characterize the TEB nonlinear calibration coefficients. At the end of the BB WUCD, the BB temperature is set back to its nominal operational temperature with the BB heater enabled and controlled. The entire process, including the time at the intermediate steps (temperatures), takes about 2.5 days.

The MODIS on-board BB is primarily used as the TEB on-orbit calibration source. A quadratic algorithm (Eqn. 1), that relates the BB path radiance and detector response, is applied on a scan-by-scan basis for each spectral band, detector, and scan mirror side.

$$\Delta L_{BB} = a_0 + b_1 \cdot dn_{BB} + a_2 \cdot (dn_{BB})^2. \quad (1)$$

The offset and nonlinear terms, a_0 and a_2 , in Eqn. 1 were initially derived during pre-launch calibration and are updated on-orbit as needed. Only the dominant linear term, b_1 , is computed on a scan-by-scan basis. The BB path radiance (ΔL_{BB}) is the difference between the

sensor at aperture radiance when viewing the on-board BB and that when viewing the SV. It includes the thermal emission contributions from the BB, scan mirror, and instrument scan cavity (reflected from the BB). Similarly, the detector response in digital number (dn_{BB}) is the difference between the averaged raw counts (digital numbers) of its BB view (50 samples) and that of its SV view (50 samples). They can be expressed by

$$\Delta L_{BB} = RVS_{BB} \cdot \epsilon_{BB} \cdot L_{BB} + (RVS_{SV} - RVS_{BB}) \cdot L_{SM} + RVS_{BB} \cdot (1 - \epsilon_{BB}) \cdot \epsilon_{CAV} \cdot L_{CAV}, \quad (2)$$

and

$$dn_{BB} = \langle DN_{BB} \rangle_{AVG} - \langle DN_{SV} \rangle_{AVG}. \quad (3)$$

where RVS_{BB} and RVS_{SV} are the response versus scan-angle (RVS) when the scan mirror views the BB and SV. The response is view angle dependent and the inclusion of the RVS terms is needed to account for the scan mirror observing the BB and SV at different angles. ϵ_{BB} and ϵ_{CAV} are the BB and scan cavity emissivity. L_{BB} , L_{SM} , and L_{CAV} are the on-board blackbody (BB), scan mirror (SM), and scan cavity (CAV) spectral radiances, which are computed at their corresponding temperatures using the Planck equation weighted over each detector's relative spectral response (RSR). Periodic BB WUCD processes provide detector responses at different temperatures and radiances, from which the offset and quadratic terms in the calibration equation can be evaluated and updated if necessary. The BB WUCD process has enabled the TEB detector noise characterization to be made at different temperatures. Figure 4 is an example illustrating detector response versus BB temperatures and radiances for Terra MODIS bands 20 and 31 (middle detector) with data from the BB WUCD process illustrated in Figure 3. The curvature in Figures 4a and 4c is due to the Planck function relationship between radiance and temperature.

Table 3 is a summary of the number of Terra and Aqua MODIS BB WUCD operations executed from launch to present. Except for the first year of the Terra mission, the BB WUCD

cycle is performed on a quarterly basis. Additional operations can be made on an as needed basis, as in the case of Terra 2006 and Aqua 2007. For Terra MODIS, there were a number of changes in its operational configuration and special tests designed to investigate SWIR electronic cross-talk behavior at the mission beginning. Because of this, there are many additional BB WUCD activities for Terra MODIS in 2000. The BB operations listed in Table 3 are only those that involve the complete WUCD process, covering a BB temperature range of 270K to 315K. A number of partial operations using a limited temperature range (without an initial cool-down process) were also performed early in the Terra mission for special testing purposes.

IV. MODIS OBC BB On-orbit Performance

A. Short-term stability and temperature uncertainty

For sensor nominal operation the BB temperature used for TEB calibration is the average over its 12 thermistors. An outlier rejection algorithm is also applied to exclude any large random telemetry noise from the average. To evaluate BB short-term stability we analyze the scan-by-scan sensor engineering data, which contains the measured temperatures from each thermistor. Figure 5 shows examples of the scan-by-scan temperatures for Terra MODIS BB thermistor 2, 6, and 10 for one 5 minute data granule from September 2003 (a) and September 2008 (b). It can be seen that the scan-to-scan variation is within $\pm 25\text{mK}$ for each individual thermistor (1 sigma). Slight differences are expected between individual thermistors. The 2003 and 2008 plots in Figure 5 show similar temperature variations, demonstrating that the scan-to-scan behavior of the Terra MODIS BB thermistors has remained nearly constant. Similar plots for Aqua MODIS BB thermistor 2, 6, and 10 are provided in Figure 6. By comparison, the scan-by-scan variation of the Aqua MODIS BB thermistors is within $\pm 10\text{mK}$. The difference among

all 12 Aqua MODIS thermistors is also smaller than that of Terra MODIS. Like Terra MODIS, Figure 6 shows little difference between the 2003 and 2008 plots for the individual BB thermistors in Aqua MODIS. The results from both instruments demonstrate that the temperature control capability designed for the MODIS BB functions well and leads to excellent stability in BB temperature on a scan-by-scan basis.

Figure 7 shows both Terra and Aqua MODIS BB temperature short-term stability for all thermistors and their average using measurements made over an entire orbit, including both daytime and nighttime granules, for similar dates in 2003 through 2008. Both instruments were in nominal operational mode with the BB at their operational set points. The Terra MODIS analysis includes only data collected with the instrument in its current electronics/formatter configuration (since day 260 of 2002). The typical variation within one orbit for each individual Terra MODIS BB thermistor is generally around 25-30mK. For the BB average temperature used in the TEB calibration, the variation is much smaller, about 10mK. As with the scan-by-scan results in Figure 6, the Aqua MODIS BB thermistors demonstrate better performance and stability over one orbit compared to Terra MODIS. The 12 Aqua MODIS BB thermistors have a typical variation of around 10mK over an entire orbit, with a BB average temperature variation of less than 5mK. The Aqua MODIS thermistor variations are seen to be more consistent over the instrument lifetime, whereas the Terra MODIS thermistors show larger year-to-year differences, but with no distinct pattern. The year-to-year differences are expected, since the BB heater needs to toggle between on and off more frequently when the BB temperature is set at a higher temperature.

Figure 8 demonstrates the BB temperature short-term stability at different operating temperatures (280K, 285K, 290K, and 315K) derived from 5 min data granules during the 4 BB

WUCD operations in 2003. As expected, the BB temperature is more stable at lower operating temperatures. For Terra MODIS, individual thermistor variability is approximately 18mK at 280K, 24mK at 285K, 27mK at 290K, and 70-100mK at 315K. The BB average temperature variation is approximately 10mK for the three lower operating temperatures and 30mK for the highest operating temperature. Overall Aqua MODIS BB performance at different operating temperatures is also better than Terra MODIS. The Aqua MODIS individual thermistor variation is about 7mK at 280K, and increases to about 10mK at 285K, 12mK at 290K and 30mK at 315K. The variability of Aqua MODIS BB average temperature is typically less than 5mK at lower operating temperatures and 10mK at higher temperatures. The demonstrated stability in short-term performance during nominal operation of the BB for both Terra and Aqua MODIS is reflected in the stability of the TEB calibration, which is performed on a scan-by-scan basis using the average BB temperature.

B. Long-term performance

The BB long-term performance for Terra MODIS is shown in Figure 9 using the daily averaged BB temperatures over the instrument lifetime from 2002 to present. Early in the mission, Terra MODIS experienced several anomalies that required switching between the primary and redundant electronics and formatter [13]. It can be seen from Figure 9 that the long-term trend has been stable, despite small seasonal variations of approximately $\pm 10\text{mK}$. For more than 6 years, the BB temperature drift is less than 15mK. The small increasing trend of BB temperature is primarily due to the slow increase of instrument and scan cavity temperatures. Because of this, the magnitude of the seasonal variations has become smaller. There is a small but noticeable temperature jump of less than 10mK around day 2002.550. This is caused by an

instrument anomaly resulting in the Solar Diffuser door becoming fixed in an open position, and thus causing an increase in instrument temperature. As a result of this anomaly and slightly higher ambient environment the BB thermistor response also increased on average by nearly 1 DN. As shown in Figure 2, 1 DN at 290K produces a temperature difference of about 13mK, which is consistent with the temperature jump seen in Figure 9. Out-of-family points that coincide with OBC activities (e.g. BB WUCD and SRCA operations) are not included in the BB temperature trend.

A similar long-term trend of BB performance for Aqua MODIS is shown in Figure 10. Unlike Terra MODIS, Aqua MODIS has operated under the same configuration (both analog and digital electronics) since launch [16]. It can be seen that the day-to-day BB performance for Aqua MODIS has been extremely stable over the instrument lifetime. There are essentially no seasonal variations like those seen for Terra MODIS, partly due to the Aqua MODIS BB having a lower operational temperature – closer to instrument ambient – and thus more easily controlled. Similar to Figure 9, the BB temperatures during BB WUCD and SRCA operations are excluded. As expected, based on the short-term performance results discussed previously, the Aqua MODIS long-term performance is better than that of Terra MODIS. The long-term drift over a 6-year period is less than 5mK in Aqua MODIS. Clearly, the BB performance of Aqua MODIS is better than Terra MODIS.

C. BB temperature uniformity and impact on calibration

As described in Section 2, the 12 BB thermistors are uniformly embedded in the BB substrate with two rows of 6 thermistors in the along-scan direction. Detectors in each spectral band are aligned in the track direction. As a result, the BB temperature uniformity and associated

impact on the calibration in the track direction can be evaluated using response differences of the individual detectors. Similarly, the impact on the scan direction can be examined using detector responses over the entire BB sector, from which 50 samples are collected. As the scan mirror rotates, the projected footprint of each pixel moves across the BB panel in the scan direction. An example of the individual thermistor temperature differences from the average BB temperature during a Terra MODIS WUCD activity is shown in Figure 11. Initially, the BB is in nominal operating mode and the observed differences between the thermistors are consistent with the scan-by-scan results shown in Figure 5. The first cool-down period to instrument ambient begins at about 204.4 (day of 2003), as seen in Figure 3, and during this time the BB heater is switched off. The BB cool-down operation is a passive process. As expected, the BB temperature is very uniform over the entire BB panel and this is reflected in the stable and consistent performance of all 12 thermistors while the BB cools. The active warm-up process (beginning at about 205.1 in Figure 11) involves the use of the BB heater with its power being switched on and off in order to control the BB at the set temperatures. This heating of the BB results in temperature gradients in the BB substrate and this can be seen in the larger temperature differences among the 12 thermistors during the warm-up activity. The largest peak-to-peak temperature difference is approximately 0.2K when the BB is operated at its highest temperature set point of 315K. The second cool-down process is again evident by the stable thermistor temperature differences before the BB is returned to its nominal operations.

The impact due to BB temperature uniformity on the TEB calibration is examined using the detector linear calibration coefficients (b_1) derived scan-by-scan during the WUCD operation. As expected, there are inherent gain differences among the detectors of a given band and the TEB calibration is therefore performed on a detector-to-detector basis. Since the BB

temperature is very uniform when the heater is off during the cool-down process, initial gain differences among individual detectors are normalized to their corresponding cool-down values. To illustrate the relative response differences among individual detectors, Figure 12 shows the granule averaged b_1 coefficient normalized by the coincident band averaged b_1 over the entire WUCD activity for all 10 detectors of band 22 (3.96 μm). The largest differences were typically between the edge detectors 1 and 10. For band 22, the relative difference is within $\pm 0.4\%$ over the entire WUCD period for the edge detectors and it becomes much smaller for the other detectors. A 0.4% response difference for band 22 is equivalent to a difference of 0.1K at its typical temperature (300K) retrieval (Table 1). A similar impact analysis for Terra MODIS band 31 (11.03 μm) is illustrated in Figure 13. It is evident that the response differences are much smaller for the detectors of band 31 than band 22 during the entire BB WUCD. This is expected since the same temperature difference in this temperature range yields a smaller radiance difference (%), thus a smaller response difference (%), at the band 31 wavelength than at the band 22 wavelength. The largest band 31 relative differences are well within $\pm 0.07\%$, which is equivalent to a difference of 0.024K at its typical temperature (300K) retrieval.

As a comparison, the Aqua MODIS BB temperature uniformity impact is also examined and presented in Figures 14-16. As illustrated in Figure 14, the Aqua MODIS BB temperature uniformity is slightly better than Terra MODIS. The relative temperature differences among individual thermistors at higher temperatures are less than 0.16K, compared to 0.2K for Terra MODIS. The detector response differences for Aqua band 22 seen in Figure 15 have more variation than those of Terra, but are within the same relative difference envelope ($\pm 0.5\%$) over the entire WUCD period. Figure 16 shows that Aqua band 31 relative response differences are

within $\pm 0.05\%$, which are smaller than those of Terra band 31. Figure 16 also reveals some small orbit-to-orbit variations.

Each scan, MODIS collects 50 samples (or frames) over the BB sector. Any systematic temperature gradient in the scan direction can be examined using detector response on a frame-by-frame basis for each scan. Figure 17a shows the along-scan impact on the TEB calibration due to BB temperature gradient for Terra MODIS band 22 detector 7 using its frame-by-frame BB responses normalized to the scan average for the five stable temperature plateaus of a WUCD activity. At 270K when the BB heater is off and the BB plate has stabilized at the ambient temperature, no difference is seen over the surface of the BB. As the temperature plateaus reach higher temperatures a gradient is observed from detector response to the BB, reaching a maximum for the 315K plateau when the BB heater is operating at maximum power. For Terra band 22 detector 7 the equivalent temperature differences between the first and last frames are equivalent to 17mK at the nominal BB operating temperature of 290K and 43mK at 315K. Similar response differences for Terra MODIS band 31 detector 7 are illustrated in Figure 17b. The comparable response of Aqua MODIS band 22 detector 7 and band 31 detector 7 are seen in Figures 18a and 18b, respectively. As expected the Aqua MODIS BB behavior is similar to that of the Terra BB but with smaller differences along track. The equivalent temperature differences between the first and last frames are 4mK at the nominal BB operating temperature of 285K and 13mK at 315K for band 22 and 7mK at 285K and 27mK at 315K for band 31. All other bands and detectors also show similar gradient patterns.

D. Validation of MODIS BB performance

MODIS BB performance and calibration impacts are examined using the long-term stability of the calibration coefficient b_1 and brightness temperature observed at the top of atmosphere (TOA). Figures 19 and 20 show that the variations of b_1 for the spectral bands on the SMIR FPA (bands 20-25) are within $\pm 0.5\%$ from 2002 to present. Terra bands 27 to 30 on the LWIR FPA show a b_1 increase of nearly 5% since 2002, whereas on Aqua, these bands are more stable. Clearly, this increase is not directly caused by the performance of the MODIS on-board BB. The remaining LWIR bands (31-36) have demonstrated stable b_1 performance for both Aqua and Terra MODIS. The vertical dashed line for Terra indicates the time period of a spacecraft anomaly and instrument safe mode. After returning to science mode it is not unusual to see changes in the b_1 response, such as the nearly 2% step change observed in bands 31 to 36. The MODIS Characterization Support Team (MCST) has used two approaches to track the stability and consistency of the atmospheric window bands (31 and 32). The first approach uses a third sensor as a transfer radiometer to inter-compare Terra and Aqua MODIS [22-23]. To reduce the uncertainty of comparison data, simultaneous nadir observations (SNO) of MODIS and the reference sensor are used. Results obtained using the NOAA-KLM series AVHRRs show that the measurements of the Terra and Aqua atmospheric window bands are very consistent with differences within 0.10K over scene temperatures of 250 to 280K [23]. The second approach uses simultaneous MODIS and ground observations at Dome Concordia (Dome C), Antarctica [24]. The high elevation and homogeneous surface characteristics of Dome C combined with the typically clear dry atmosphere make the site ideal for remote sensor performance validation. Observations at very low temperatures in the Antarctic winter ($\sim 200\text{K}$) help to identify sensor calibration problems since they are well below the BB calibration temperatures. Using the ground temperature measurement at Dome C as a proxy for comparison, the relative bias

between Terra and Aqua MODIS was confirmed to be within 0.10K for bands 31 and 32, a close agreement with that found using the first approach. The bias displays no obvious drift over the period of 2002 to 2007 [24].

MODIS BB on-orbit performance has also been validated using the accuracy and quality of its key TEB data products, such as land surface temperature (LST) and sea surface temperature (SST). Validation of the MODIS LST usually is conducted over a wider temperature range than that for SST. Uncertainties in LST data are generally higher than SST data because of the surface type and scene temperature variations. An early study using in-situ measurements obtained from field campaigns under clear-sky conditions between 2000 and 2002 showed an agreement within 1.0K for Terra MODIS in the LST range of 250.0 to 320.0K [25]. Recent validation efforts using a radiance-based approach show similar results [26]. For comparison of MODIS SST with radiometrically-derived ocean skin temperatures from ships and bulk measurements from buoys, results have indicated that both Terra and Aqua MODIS SST have a very low mean bias error of 0.10K [27]. Another study uses surface radiances measured from an automated site established at Lake Tahoe from 2000 to 2005 to validate MODIS TEB on-orbit calibration. The surface radiances are converted to predicted at-sensor radiances with atmospheric radiative transfer models, which are then used to make absolute comparison with MODIS measured at-sensor radiances. Results show that the percent differences between the predicted and measured at-sensor radiances for MODIS Terra bands 31 and 32 are 0.04% and 0.15%, corresponding to temperature differences of 0.05K and 0.10K, respectively [28].

V. Lessons from MODIS On-board BB Operation and Calibration

MODIS is an Earth-observing spectral radiometer that is equipped with a BB capable of being actively operated and controlled over of a wide range of temperatures. This feature has allowed the sensor calibration to be performed at different temperatures and, therefore, its on-orbit performance to be examined more thoroughly. From extensive pre-launch calibration and characterization of MODIS on-board BB, and its on-orbit operation and performance over the Terra and Aqua missions, there have been a number of lessons learned. They are briefly summarized in the following:

- Complete and accurate pre-launch calibration and characterization of sensor on-board BB emissivity are critical as TEB calibration and data product quality strongly depend on the accuracy of radiance calibration and the BB is the dominant term among all the calibration sources (Eq. 2). In addition to the standard modeling approach, end-to-end measurements should be made to validate the BB emissivity and its uncertainty with reference to a high quality ground-based BB calibration source. The uncertainty in the BB emissivity will cause a systematic calibration error of nearly the same percentage for each spectral band. For the same reason, the BB thermistors should be fully characterized with temperature traceability to NIST standards.
- The on-board BB should be fully characterized pre-launch at all design configurations. The impact on BB temperature control and thermistor stability varies with different configurations and electronics. For Aqua MODIS, the B-side electronics configuration demonstrates better performance of the on-board BB, as shown in this study. The decision to use the B-side electronics configuration as the Aqua MODIS at launch configuration was based on the extensive calibration efforts made pre-launch and lessons learned from Terra MODIS on-orbit experience.

- The on-board BB nominal operating temperature should be carefully selected by considering all factors which could impact calibration quality. When the BB is set at a higher temperature, the relative contributions from other source terms, which, typically, are less accurately characterized, become much smaller (Eq. 2). On the other hand, the random noise (or digitization errors) of the BB thermistors and the BB panel non-uniformity increase more rapidly when the BB operating temperature is above 300K.
- Even if all thermistors are characterized with reference to NIST standards, their performance varies. Because of the random noise in each individual BB thermistor, multiple well characterized thermistors should be used together to accurately determine the BB temperature. The number of thermistors should be based on the size of the BB panel and its operating environment. Potential non-uniformity of the BB, when it is actively controlled above the instrument ambient, can also be evaluated using different thermistors embedded across the BB substrate. As shown in this study, the calibration impact due to BB non-uniformity and thermistor random noise are generally small since MODIS TEB calibration uses the average BB temperature and the detector scan-by-scan response averaged over all 50 frames across the BB sector. However, the impact due to BB non-uniformity needs to be more carefully considered for high spatial resolution radiometers.

VI. Summary

This paper provides a comprehensive analysis of MODIS BB on-orbit operation and performance. Results derived from sensor telemetry and response show that both Terra and Aqua MODIS BB have continued to function well throughout each instrument's lifetime. In general, Aqua MODIS BB performs better than Terra MODIS in terms of its short-term and long-term

temperature stability and thermistor noise characteristics. Typical BB temperature uncertainty is less than 10mK for Terra MODIS at the nominal operational temperature of 290K and about 5mK for Aqua MODIS at its operational temperature of 285K. The impact due to MODIS BB temperature uncertainty on the TEB calibration is extremely small compared to the sensor specified calibration requirements. It is clear that the MODIS on-board BB has provided and will continue to provide a stable and reliable calibration reference for all the thermal emissive bands and, consequently, will enable continued high quality science data products to be derived from its thermal emissive bands. Lessons learned from the design, operation and performance of the MODIS BB should be considered in the development of next-generation thermal infrared sensors.

Acknowledgement

The authors would like to thank Na Chen, Kwo-Fu Chiang, and Sriharsha Madhavan of the MODIS Characterization Support Team (MCST) for technical assistance and contributions to the analysis.

References

1. V.V. Salomonson, W.L. Barnes, X. Xiong, S. Kempler, and E. Masuoka, "An Overview of the Earth Observing System MODIS Instrument and Associated Data Systems Performance," *Proceedings of IGARSS*, 2002.
2. W.L. Barnes and V.V. Salomonson, "MODIS: A global image spectroradiometer for the Earth Observing System," *Critical Reviews of Optical Science and Technology*, CR47, 285-307, 1993.
3. C.O. Justice, E. Vermote, J.R.G. Townshend, R. Defries, D.P. Roy, D.K. Hall, V.V. Salomonson, J.L. Privette, G. Riggs, A. Strahler, W. Lucht, R.B. Myneni, P. Lewis, and M.J. Barnsley, "The Moderate Resolution Imaging Spectroradiometer (MODIS): Land Remote Sensing for Global Change Research," *IEEE Trans. Geosci. Remote Sensing*, 36, 1228-1249, 1998.
4. W.E. Esaias, M.R. Abbott, I. Barton, O.W. Brown, J.W. Campbell, K.L. Carder, D.K. Clark, R.L. Evans, F.E. Hoge, H.R. Gordon, W.P. Balch, R. Letelier, and P.J. Minnett, "An Overview of MODIS Capabilities for Ocean Science Observations," *IEEE Trans. Geosci. Remote Sensing*, 36, 1250-1265, 1998.
5. M.D. King, W.P. Menzel, Y.J. Kaufman, D. Tanre, B.C. Gao, S. Platnick, S.A. Ackerman, L.A. Remer, R. Pincus, and P.A. Hubanks, "Cloud and Aerosol Properties, Precipitable Water, and Profiles of Temperature and Water Vapor from MODIS," *IEEE Trans. Geosci. Remote Sensing*, 41, 442-458, 2003.
6. C.L. Parkinson, "Aqua: An Earth-Observing Satellite Mission to Examine Water and Other Climate Variables," *IEEE Trans. Geosci. Remote Sensing*, 41, 173-183, 2003.

7. W.L. Barnes, T.S. Pagano, and V.V. Salomonson, "Prelaunch characteristics of the Moderate Resolution Imaging Spectroradiometer (MODIS) on EOS-AM1," *IEEE Trans. Geosci. Remote Sensing*, 36, 1088-1100, 1998.
8. X. Xiong, N. Che, C. Pan, X. Xie, J. Sun, W.L. Barnes, and B. Guenther, "Results and Lessons form MODIS Reflective Solar Bands Calibration: Pre-launch to On-orbit," *Proceedings of SPIE – Earth Observing Systems XI*, Vol. 6296, 629607, doi:10.1117/12.679144, 2006.
9. X. Xiong, K. Chiang, N. Chen, S. Xiong, W.L. Barnes, and B. Guenther, "Results and Lessons from MODIS Thermal Emissive Bands Calibration: Pre-launch to On-orbit," *Proceedings of SPIE – Earth Observing Systems XI*, Vol. 6296, 62960A, doi:10.1117/12.680992, 2006.
10. X. Xiong and W.L. Barnes, "An Overview of MODIS Radiometric Calibration and Characterization," *Advances in Atmospheric Sciences*, 23 (1), 69-79, 2006.
11. X. Xiong, K. Chiang, J. Esposito, B. Guenther, and W. Barnes, "MODIS On-orbit Calibration and Characterization," *Metrologia*, 40, 89-92, 2003.
12. X. Xiong, J. Sun, W. Barnes, V. Salomonson, J. Esposito, H. Erives, and B. Guether, "Multiyear on-orbit calibration and performance of Terra MODIS reflective solar bands," *IEEE Trans. Geosci. Remote Sensing*, vol. 45, no. 4, 879-889, 2007.
13. X. Xiong, K. Chiang, A. Wu, W. Barnes, B. Guether, and V. Salomonson, "Multiyear on-orbit calibration and performance of Terra MODIS thermal emissive bands," *IEEE Trans. Geosci. Remote Sensing*, vol. 46, no. 6, 1790-1803, 2008.
14. X. Xiong, N. Che, and W.L. Barnes, "Terra MODIS On-orbit Spatial Characterization and Performance", *IEEE Trans. Geosci. Remote Sensing* 43, 355-365, 2005.

15. X. Xiong, N. Che, and W.L. Barnes, "Terra MODIS On-orbit Spectral Characterization and Performance", *IEEE Trans. Geosci. Remote Sensing*, Vol. 44, No. 8, 2198-2206, 2006.
16. X. Xiong, B. N. Wenny, A. Wu, W. L. Barnes, and V. V. Salomonson, "Aqua MODIS Thermal Emissive Band On-orbit Calibration, Characterization, and Performance," *IEEE Trans. Geosci. Remote Sensing*, 47 (3), 803-814, 2009.
17. M. Weinreb, G. Hamilton, and S. Brown, "Nonlinearity Corrections in Calibration of Advanced Very High Resolution Radiometer Infrared Channels," *J. Geophys. Res.*, 95 (C5), 7381-7388, 1990.
18. S. Kurihara, H. Murakami, K. Tanaka, T. Hashimoto, I. Asanuma, and J. Inoue, "Calibration and Instrument Status of ADEOS-II Global Imager," *Proceedings of SPIE – Sensors, Systems, and Next Generation Satellites VII*, Vol. 5234, 11-19, 2004.
19. I. M. Mason, P. H. Sheather, J. A. Bowles, and G. Davies, "Blackbody Calibration Sources of High Accuracy for a Spaceborne Infrared Instrument: the Along Track Scanning Radiometer," *Appl. Opt.*, 35 (4), 629-639, 1996.
20. B. L. Markham, W.C. Boncyk, D. L. Helder, and J. L. Barker, "Landsat-7 Enhanced Thematic Mapper Plus Radiometric Calibration," *Canadian J. Remote Sens.*, 23 (4), 318-332, 1997.
21. T. S. Pagano, H. H. Aumann, D. E. Hagan, and K. Overoye, "Prelaunch and In-flight Radiometric Calibration of the Atmospheric Infrared Sounder (AIRS)," *IEEE Trans. Geosc. Remote Sensing*, 41 (2), 265-273, 2003.
22. A. Wu, C. Cao, and X. Xiong, "Intercomparison of the 11- and 12- μm bands of Terra and Aqua MODIS using NOAA-17 AVHRR," *Proceedings of SPIE –Earth Observing Systems VIII*, Vol. 5151, 384-394, 2003.

23. X., Xiong, A. Wu, and C. Cao, "On-Orbit Calibration and Inter-Comparison of Terra and Aqua MODIS Surface Temperature Spectral Bands," *Inter. J. Remote Sens.*, 29(17), 5347-5359, 2008.
24. B. N. Wenny, and X. Xiong, "Using a Cold Earth Surface Target to Characterize Long-term Stability of the MODIS Thermal Emissive Bands," *IEEE Geosci. Remote Sensing Lett.*, 5 (2), 162-165, 2008.
25. Z. Wan, Y. Zhang, Q. Zhang, and Z.-L. Li, "Quality Assessment and Validation of the MODIS Global Land Surface Temperature," *Inter. J. Remote Sens.*, 25 (1), 261-278, 2004.
26. Z. Wan and Z.-L. Li, "Radiance-based validation of the V5 MODIS land-surface temperature product" *Inter. J. Remote Sens.*, 29(17-18), 5373-5395, 2008
27. P. J. Minnett, R.H. Evans, E. J. Kearns, and O. B. Brown, "Sea-surface temperature Measured by the Moderate Resolution Imaging Spectrometer (MODIS)," *Proceedings of IGARSS*, 2002.
28. S. Hook, R. Vaughan, H. Tonooka, and S. Schladow, "Absolute Radiometric In-Flight Validation of Mid and Thermal Infrared Data from ASTER and MODIS Using the Lake Tahoe CA/NV, USA Automated Validation Site," *IEEE Trans. Geosci. Remote Sensing*, 45 (6), 1798-1807, 2007.

Table 1. MODIS Thermal Emissive Bands Specifications

Band	CW	BW	L _{typ}	T _{typ}	L _{max}	T _{max}	NEdL	NEdT	UC (%)	UC (T)
20	3.75	0.18	0.45	300	1.71	335	0.0010	0.05	0.75	0.18
21	3.96	0.06	2.38	335	86	500	0.0154	0.20	1	0.31
22	3.96	0.06	0.67	300	1.89	328	0.0019	0.07	1	0.25
23	4.05	0.06	0.79	300	2.16	328	0.0022	0.07	1	0.25
24	4.47	0.07	0.17	250	0.34	264	0.0022	0.25	1	0.19
25	4.52	0.07	0.59	275	0.88	285	0.0062	0.25	1	0.24
27	6.72	0.36	1.16	240	3.21	271	0.0108	0.25	1	0.27
28	7.33	0.30	2.19	250	4.46	275	0.0172	0.25	1	0.32
29	8.55	0.30	9.59	300	14.5	324	0.0090	0.05	1	0.53
30	9.73	0.30	3.70	250	6.34	275	0.0219	0.25	1	0.42
31	11.03	0.50	9.56	300	13.3	324	0.0070	0.05	0.5	0.34
32	12.02	0.50	8.95	300	12.1	324	0.0061	0.05	0.5	0.37
33	13.34	0.30	4.53	260	6.56	285	0.0183	0.25	1	0.62
34	13.64	0.30	3.77	250	5.02	268	0.0161	0.25	1	0.59
35	13.94	0.30	3.11	240	4.42	261	0.0141	0.25	1	0.55
36	14.24	0.30	2.08	220	2.96	238	0.0154	0.35	1	0.47

CW: Center Wavelengths in μm ;

BW: Bandwidths in μm ;

L_{typ}: Typical Spectral Radiance in $\text{W}/\text{m}^2/\mu\text{m}/\text{sr}$

T_{typ}: Temperature at L_{typ} in Kelvin (K);

L_{max}: Maximum Spectral Radiance in $\text{W}/\text{m}^2/\mu\text{m}/\text{sr}$

T_{max}: Temperature at L_{max} in Kelvin (K);

NEdL: Noise Equivalent Radiance Difference in $\text{W}/\text{m}^2/\mu\text{m}/\text{sr}$;

NEdT: Noise Equivalent Temperature Difference in K;

UC (%): Uncertainty in %;

UC (T): Uncertainty in Temperature.

Table 2. Terra and Aqua MODIS BB Thermistor Dynamic Range

Thermistor	Terra MODIS-A		Terra MODIS-B		Aqua MODIS-A		Aqua MODIS-B	
	T _{BB_MIN}	T _{BB_MAX}	T _{BB_MIN}	T _{BB_MAX}	T _{BB_MIN}	T _{BB_MAX}	T _{BB_MIN}	T _{BB_MAX}
1	269.17	321.56	269.19	321.62	269.04	321.05	269.09	320.99
2	268.80	320.97	268.82	321.03	268.94	320.93	269.00	320.88
3	268.71	321.32	268.73	321.38	268.92	320.94	268.97	320.89
4	268.82	321.22	268.84	321.28	268.97	321.06	269.03	321.00
5	268.81	321.11	268.83	321.17	269.34	321.08	269.39	321.03
6	268.82	320.98	268.84	321.04	269.18	321.24	269.24	321.18
7	269.08	321.49	269.09	321.55	268.91	320.86	268.96	320.80
8	268.99	321.36	269.01	321.42	269.00	321.07	269.05	321.02
9	269.01	321.28	269.02	321.34	269.05	321.11	269.11	321.06
10	268.83	321.01	268.85	321.07	269.12	321.11	269.17	321.05
11	268.75	321.00	268.77	321.06	268.98	320.91	269.03	320.85
12	269.02	321.32	269.04	321.38	269.10	321.10	269.15	321.05

T_{BB_MIN}: BB minimum temperature

T_{BB_MAX}: BB maximum temperature

Table 3. Number of complete Warm-up/Cool-down BB operations executed on-orbit per year

	2000	2001	2002	2003	2004	2005	2006	2007	2008
Terra	16	4	4	4	4	4	5	4	4
Aqua	-	-	4	4	4	4	4	5	4

Figure Captions:

Figure 1 MODIS on-board blackbody

Figure 2 (a) Relationship between BB temperatures and thermistor digital numbers (DN); (b) Temperature difference due to electronic readout error of 1 DN. Data from Terra MODIS BB thermistor 6 (A-side electronics).

Figure 3 (a) Terra MODIS BB warm-up and cool-down profile (2003204-207) with BB temperatures changing from its nominal setting (290K), to instrument ambient (273K), to the maximum operational temperature (315K), to instrument ambient (273K), and back to its nominal setting (290K). (b) Similar plot for Aqua MODIS BB warm-up and cool-down profile from 2003209-211).

Figure 4 Detector response versus BB temperature and radiance for the middle detector of Terra MODIS band 22, (a) and (b); and for Terra MODIS band 31, (c) and (d). Data selected from same BB warm-up and cool-down illustrated in Figure 3.

Figure 5 Terra MODIS BB temperature (thermistor 2, 6, 10) short-term stability for one 5min data granule: (a) 2003260.0200 and (b) 2008260.0200.

Figure 6 Aqua MODIS BB temperature (thermistor 2, 6, 10) short-term stability for one 5min data granule: (a) 2003260.0200 and (b) 2008260.0200.

Figure 7 Standard deviation of the 12 thermistors and the average BB temperature for all scans collected in one orbit for each year from 2003 through 2008 for a) Terra MODIS and b) Aqua MODIS.

Figure 8 Standard deviation for one 5 minute granule at 4 temperature plateaus (280K, 285K, 290K, and 315K) during the same WUCD activity illustrated in Figure 3a and 3b for a) Terra and b) Aqua.

Figure 9 Long term trend of daily average BB temperature for Terra between mid-2002 to end of 2008. The vertical dashed line indicates the occurrence of an instrument anomaly.

Figure 10 Long term trend of daily average BB temperature for Aqua from launch to end of 2008.

Figure 11 Thermistor temperature differences from average BB temperature during the Terra WUCD cycle (illustrated in Figure 3a) on 2003204-207

Figure 12 Terra Band 22 detector linear coefficient trend during the WUCD cycle (illustrated in Figure 3a) on 2003204-207, normalized by band average coefficient. All detectors are included.

Figure 13 Terra Band 31 detector linear coefficient trend during the WUCD cycle (illustrated in Figure 3a) on 2003204-207, normalized by band average coefficient. All detectors are included.

Figure 14 Thermistor temperature differences from average BB temperature during the Aqua WUCD cycle on 2003209-211

Figure 15 Aqua Band 22 detector linear coefficient trend during WUCD cycle (illustrated in Figure 3b) on 2003209-211, normalized by band average coefficient. All detectors are included.

Figure 16 Aqua Band 31 detector linear coefficient trend during WUCD cycle (illustrated in Figure 3b) on 2003209-211, normalized by band average coefficient. All detectors are included.

Figure 17 Frame dependence of Normalized BB response at the 5 temperature plateaus of the WUCD cycle on 2003204-207 for (a) Terra band 22 detector 7, and (b) Terra band 31 detector 7.

Figure 18 Frame dependence of Normalized BB response at the 5 temperature plateaus of the WUCD cycle on 2003209-211 for (a) Aqua band 22 detector 7, and (b) Aqua band 31 detector 7.

Figure 19 Long term trend of band-averaged linear calibration coefficient for all TEB (excluding band 21) for Terra. The y-range for each band is 5%.

Figure 20 Long term trend of band-averaged linear calibration coefficient for all TEB (excluding band 21) for Aqua. The y-range for each band is 5%.

Figure 1

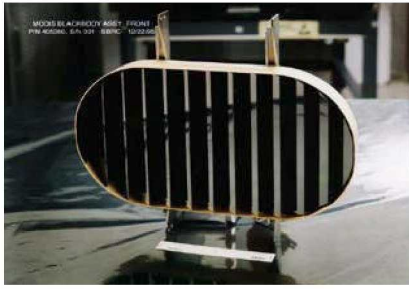
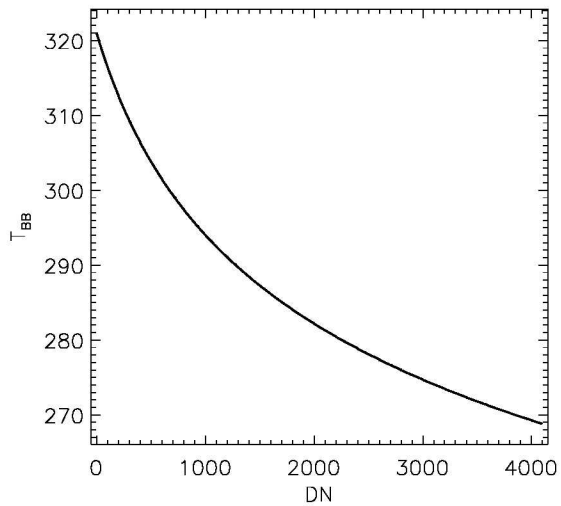
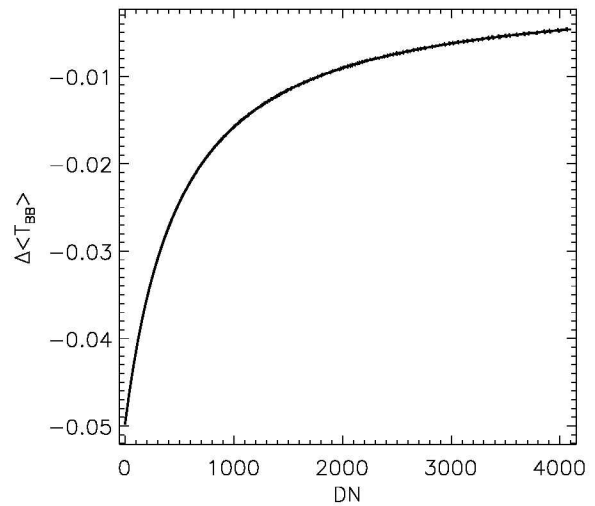


Figure 2

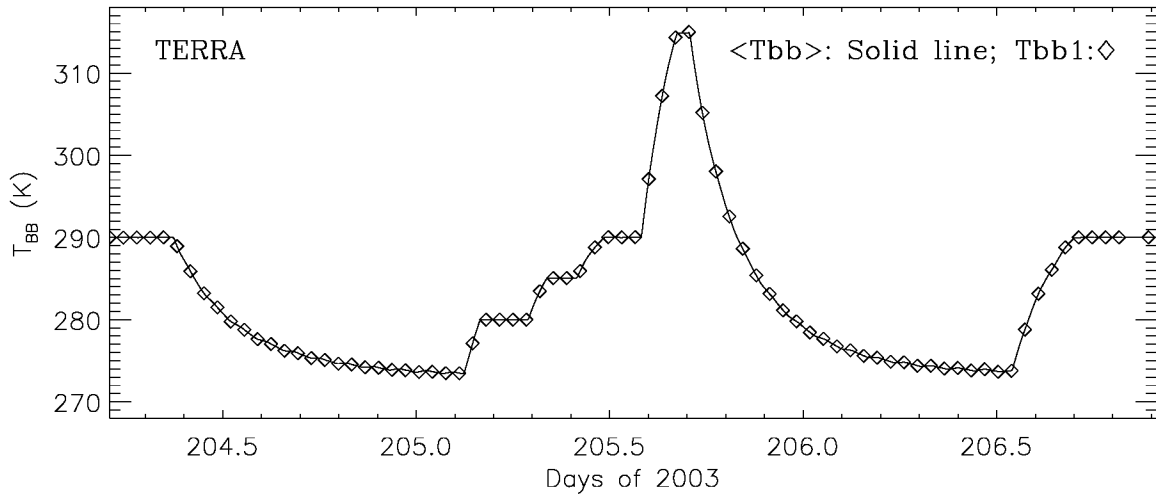


(a)

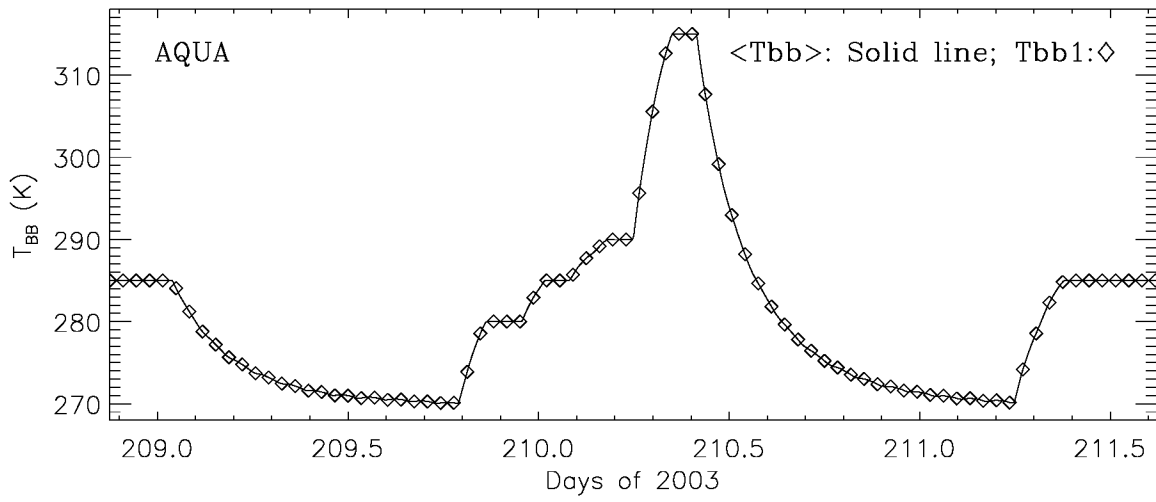


(b)

Figure 3

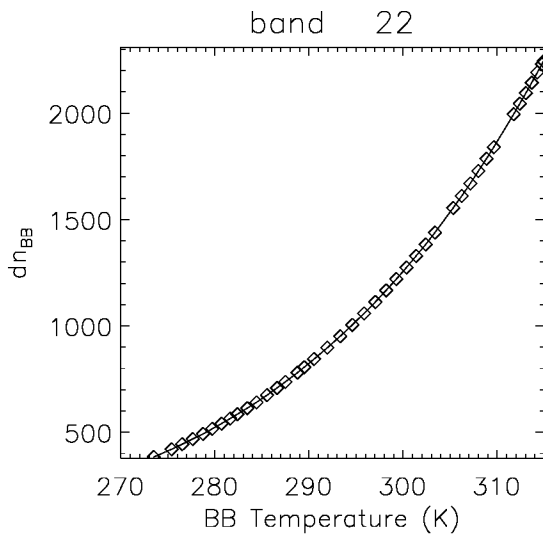


(a)

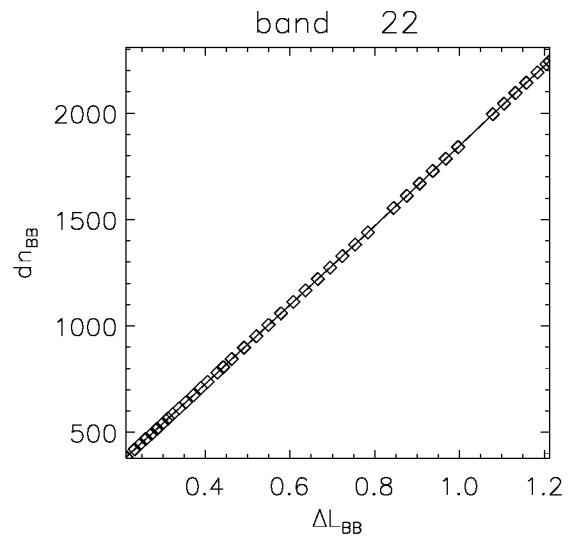


(b)

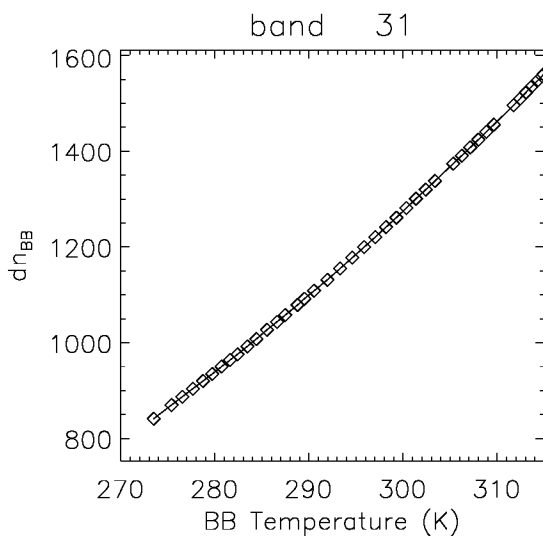
Figure 4



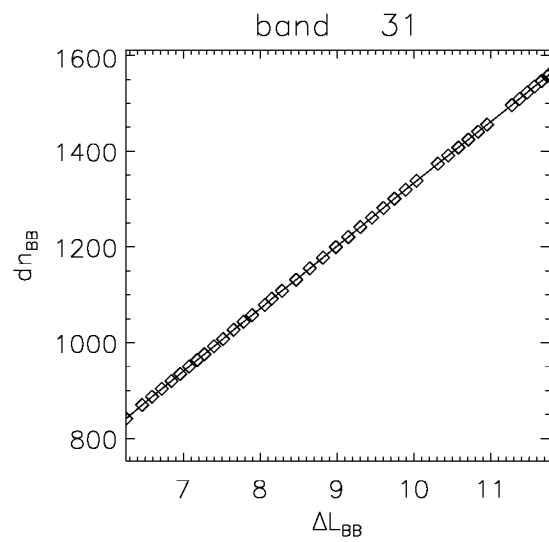
(a)



(b)

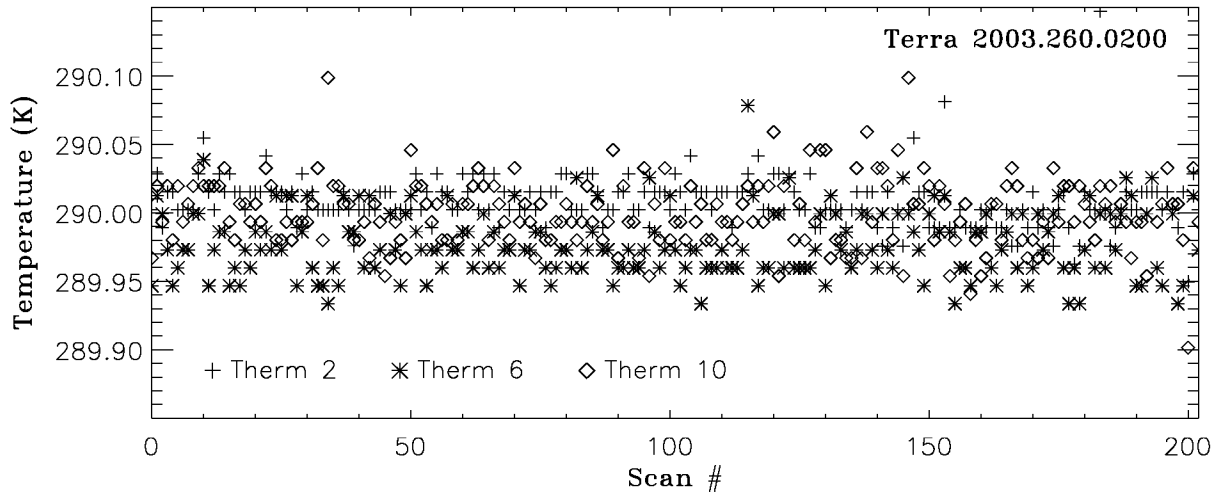


(c)

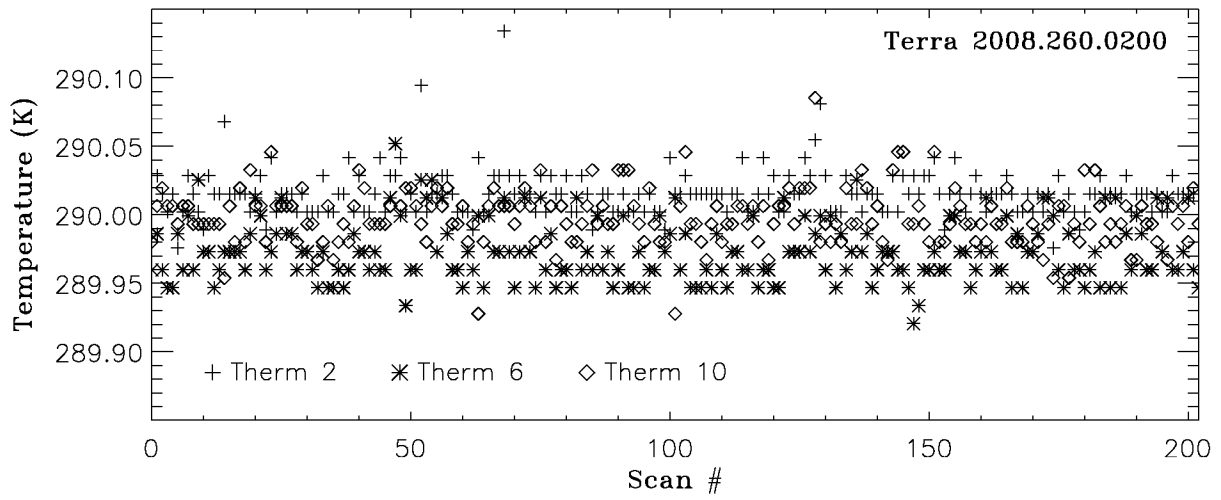


(d)

Figure 5

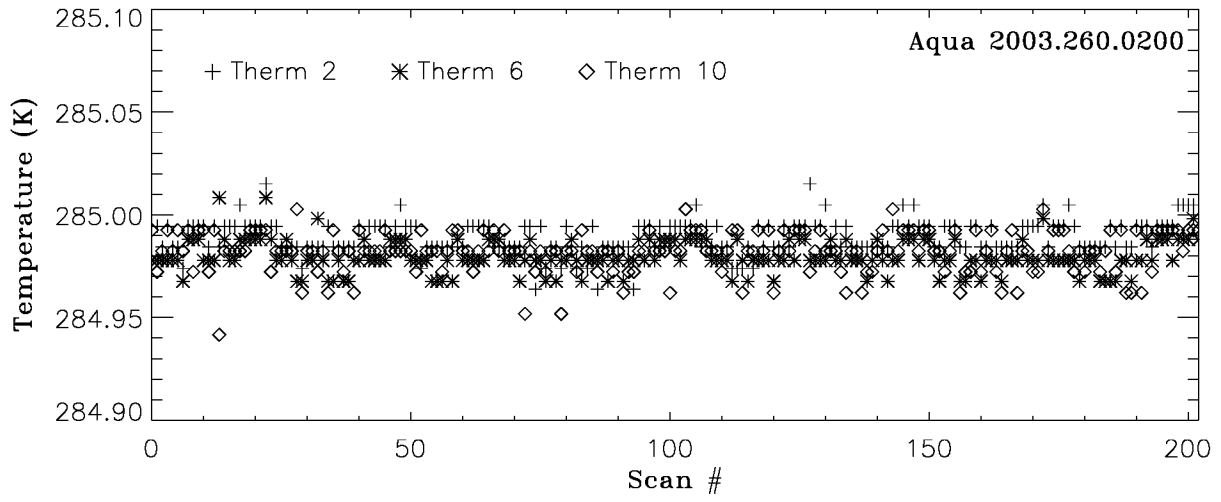


(a)

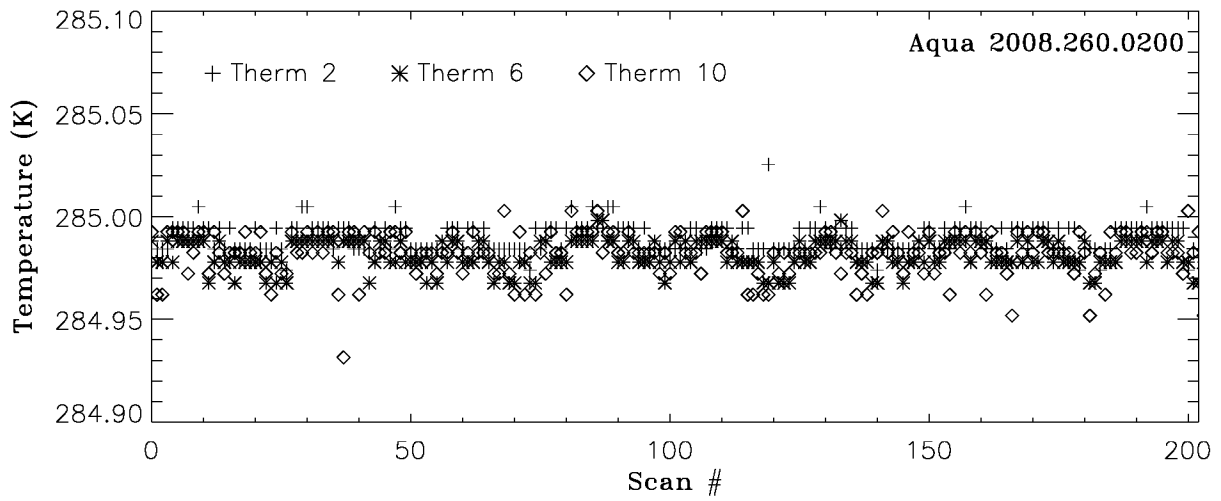


(b)

Figure 6

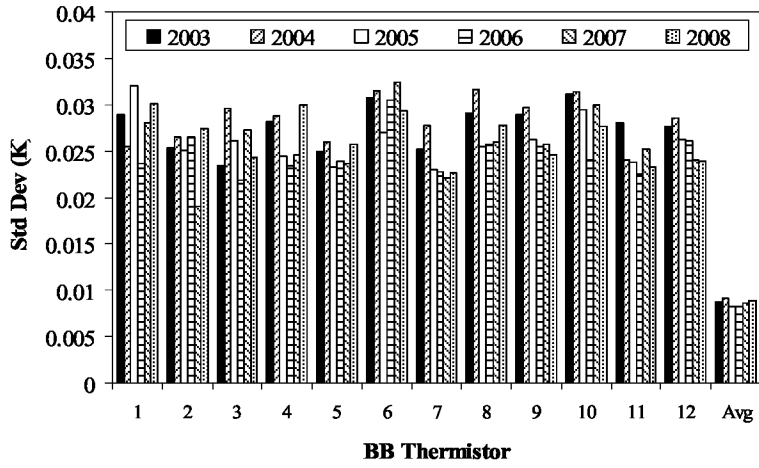


(a)

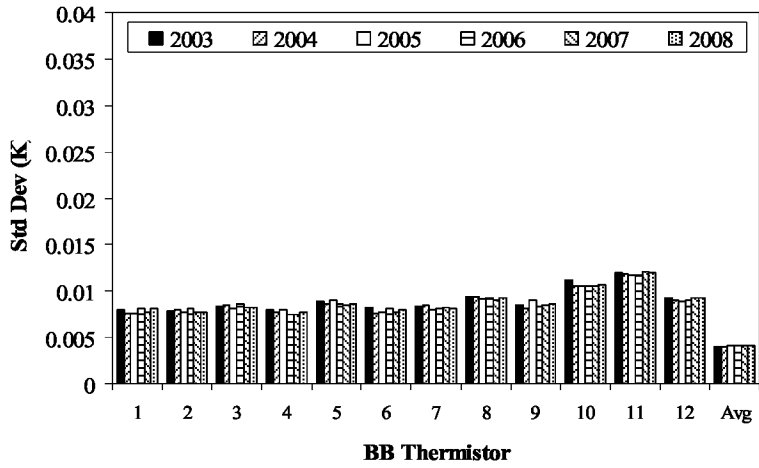


(b)

Figure 7

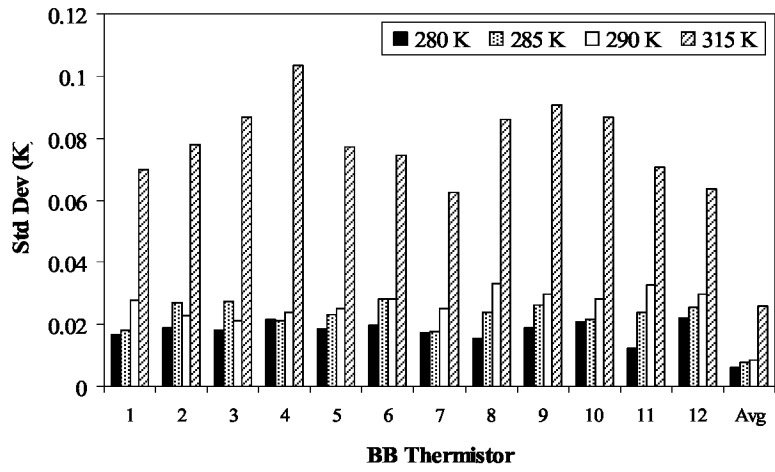


(a)

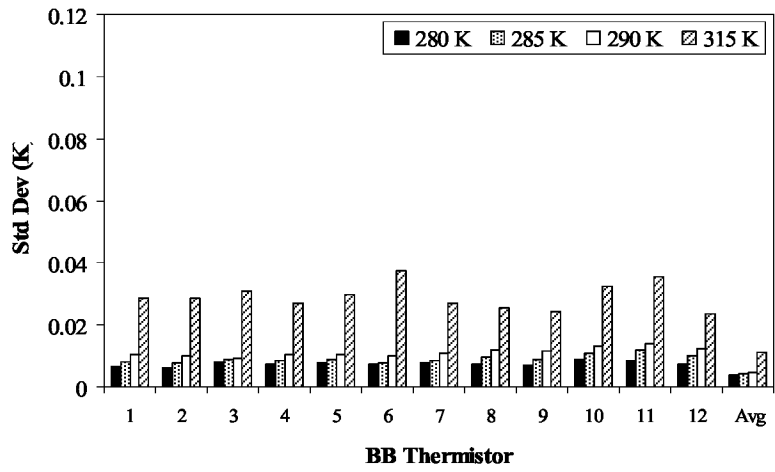


(b)

Figure 8



(a)



(b)

Figure 9

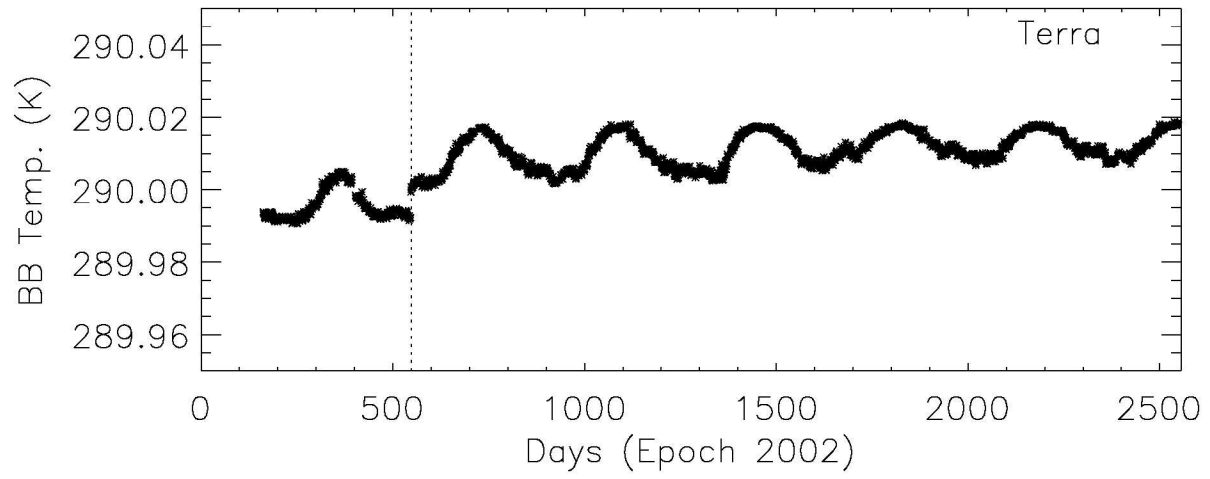


Figure 10

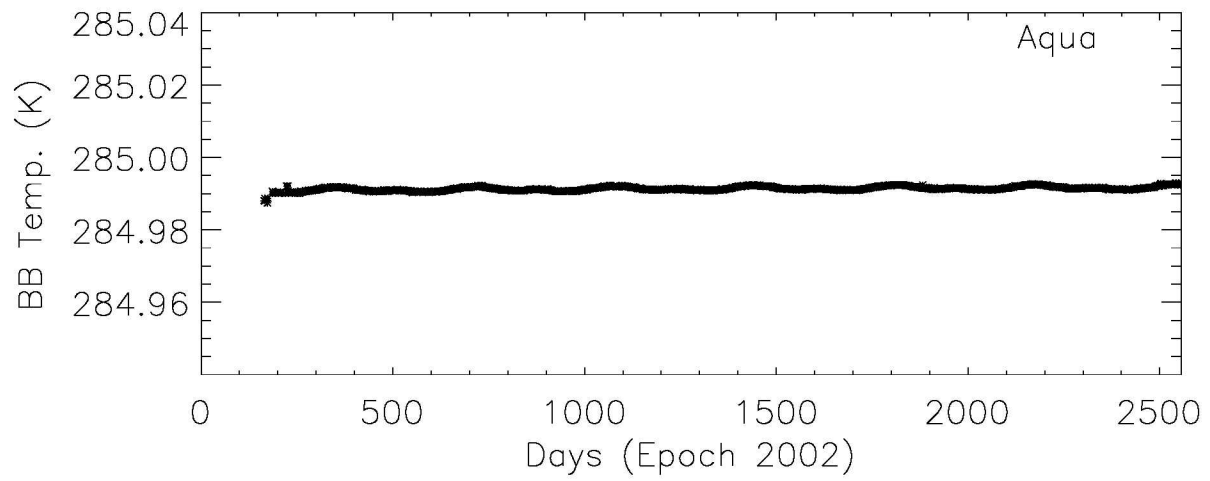


Figure 11

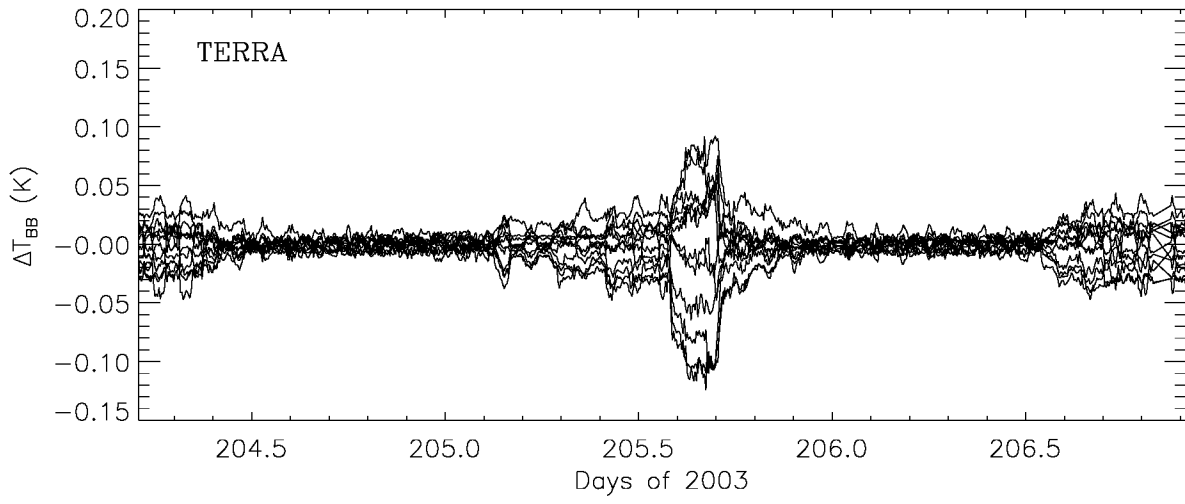


Figure 12

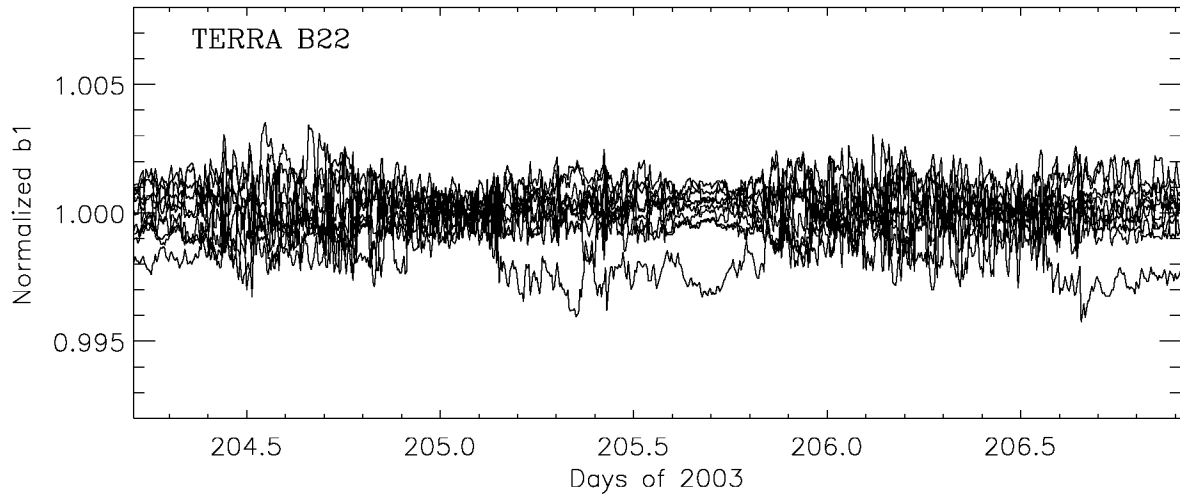


Figure 13

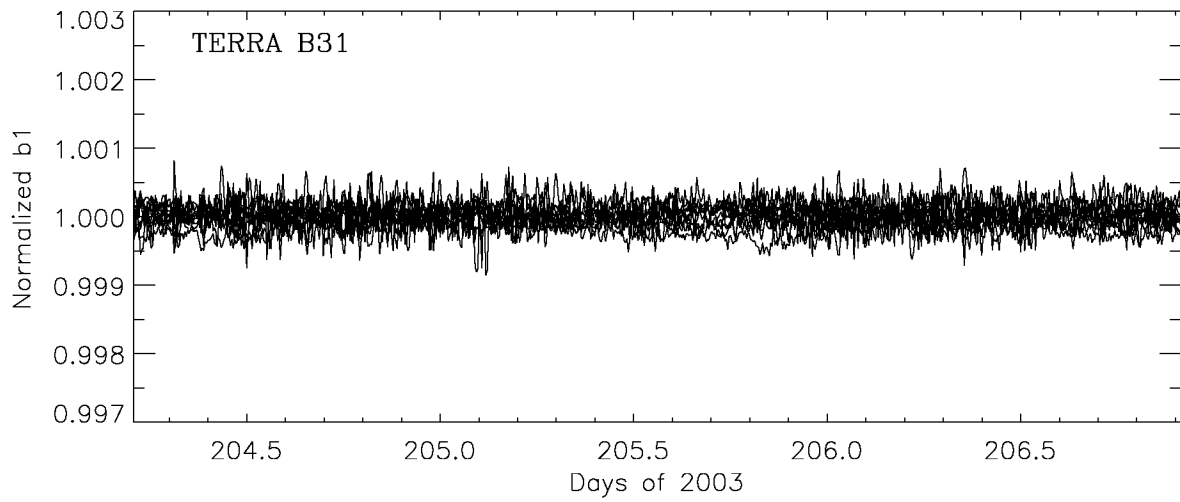


Figure 14

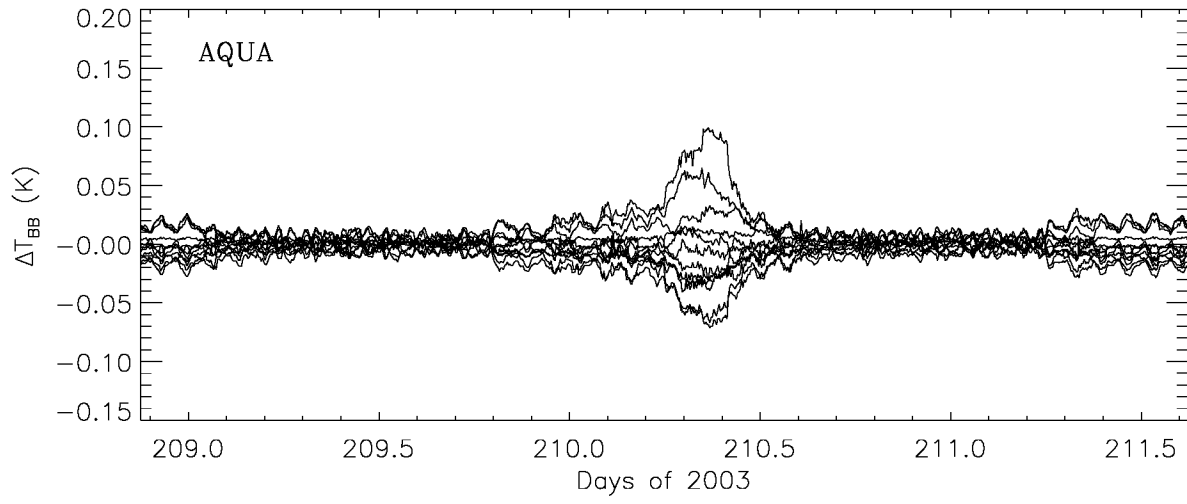


Figure 15

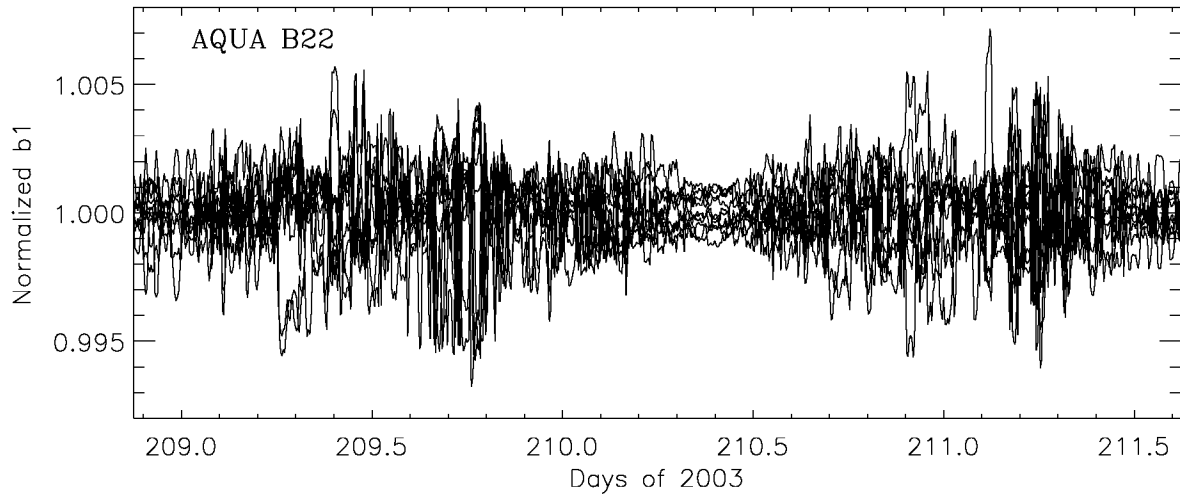


Figure 16

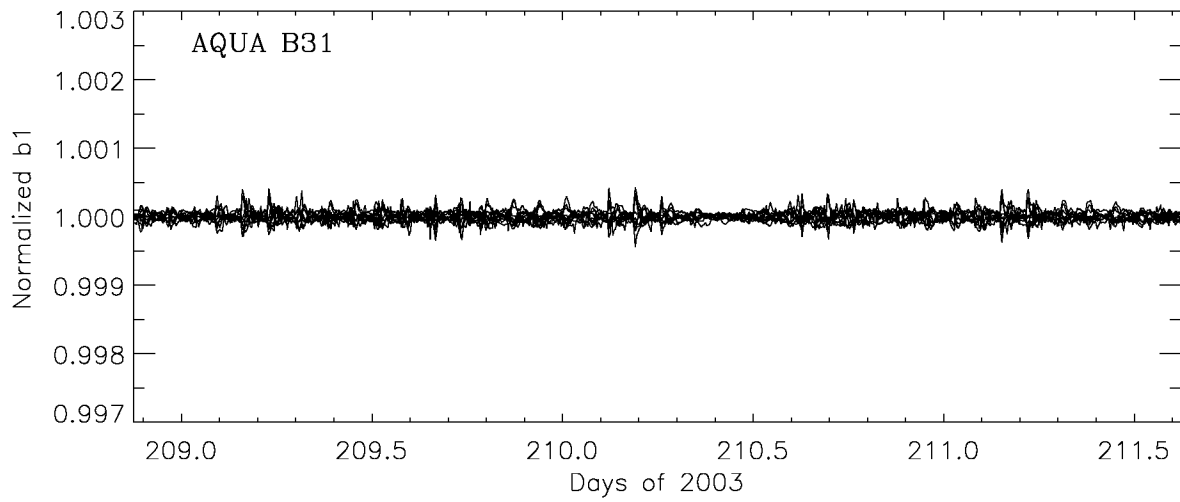
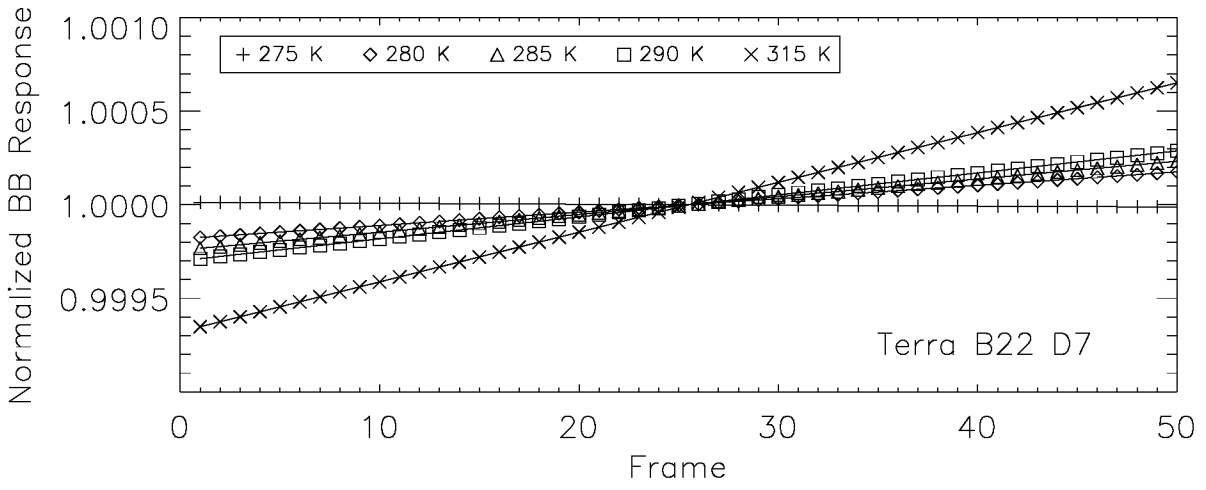
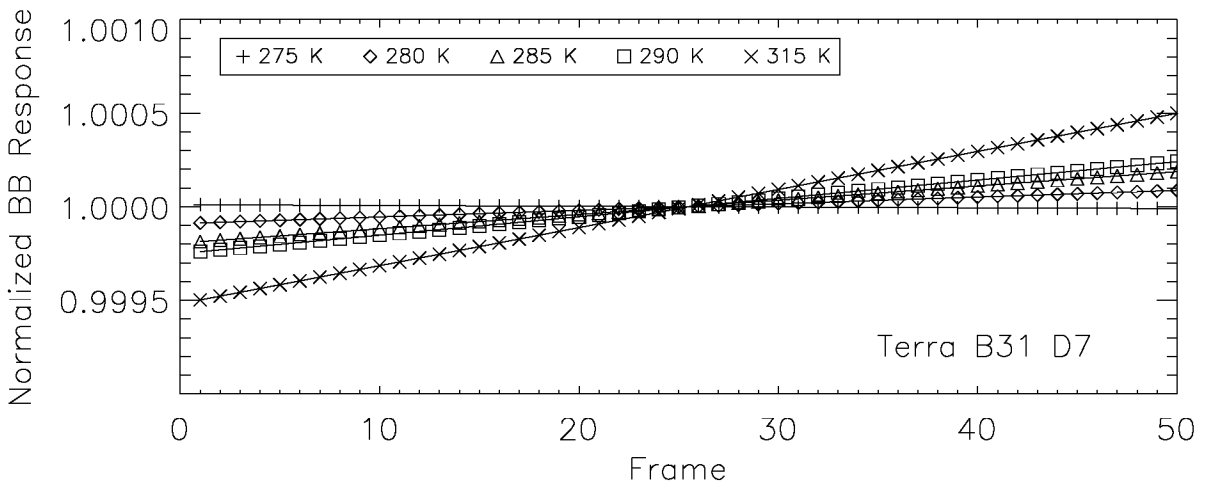


Figure 17

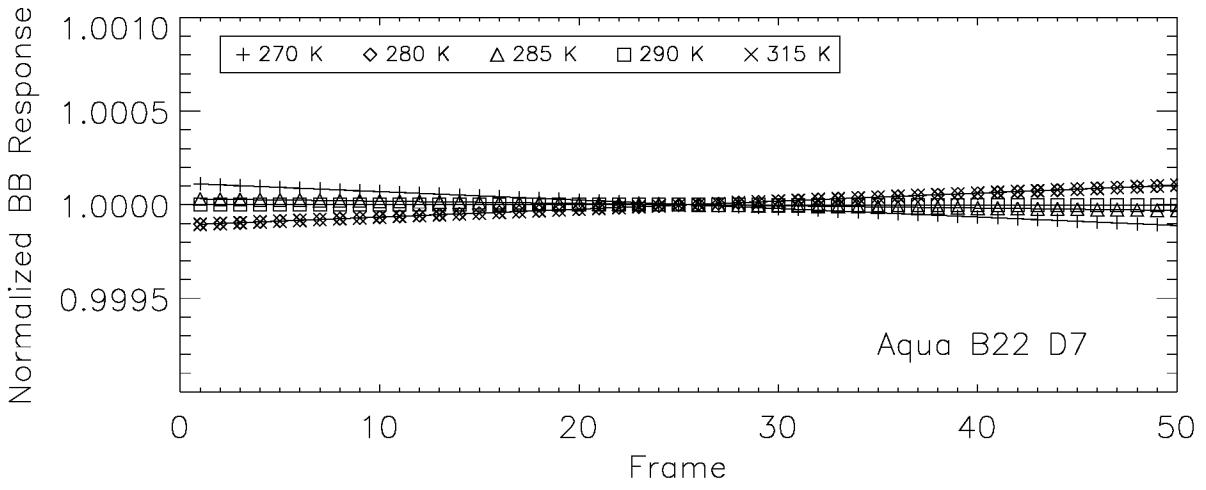


(a)

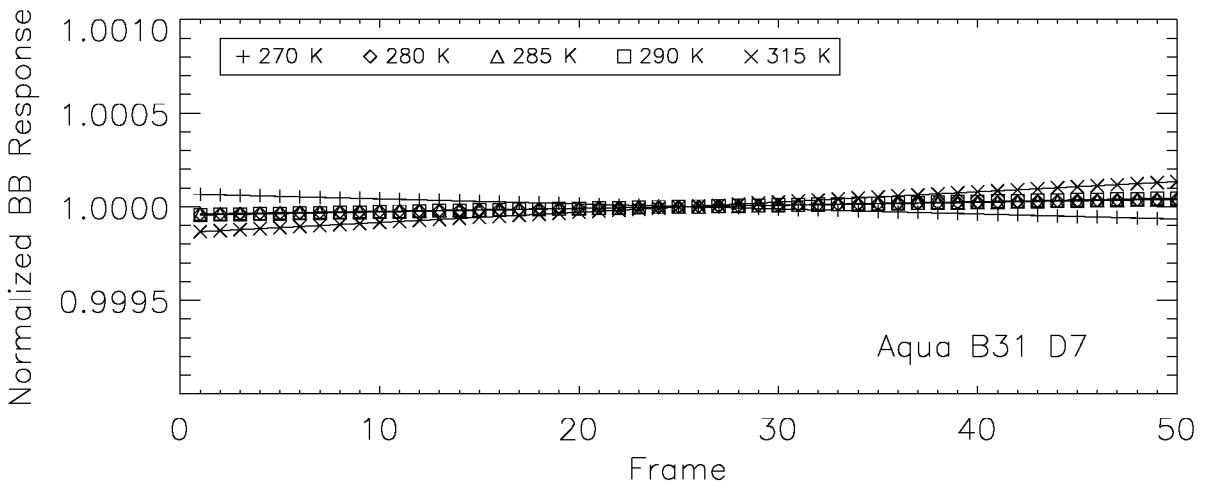


(b)

Figure 18



(a)



(b)

Figure 19

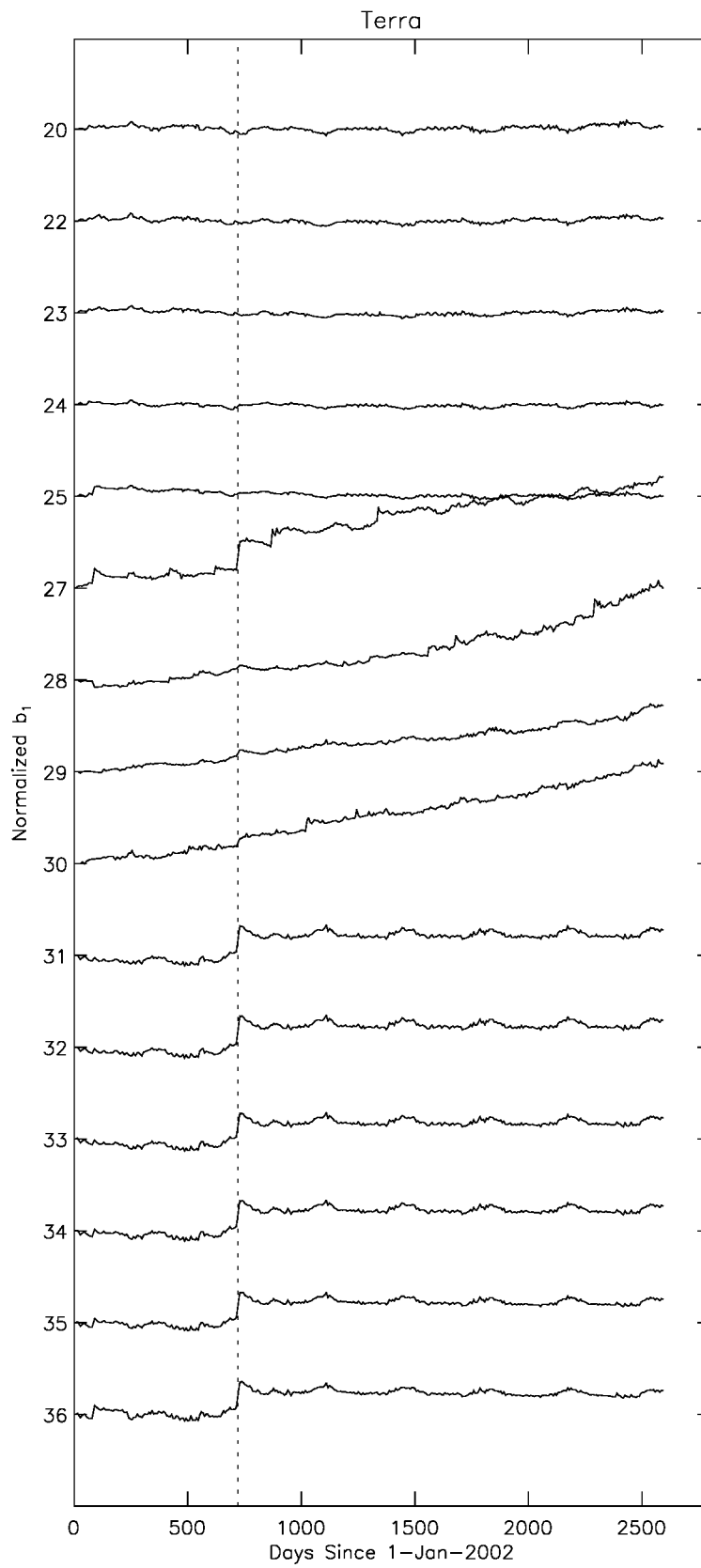


Figure 20

